

PACS: 61.05.cp, 78.20.Ci, 78.30.Fs, 78.40.Fy, 78.66.Hf

GROWTH OF EUROPIUM-DOPED MAGNESIUM SELENIDE FILMS BY ELECTRIC FIELD-ASSISTED SPRAY PYROLYSIS: OPTICAL AND STRUCTURAL ANALYSIS

 **D.M. Jeroh***,  **A.J. Ekpunobi**,  **D.N. Okoli**

Physics/Industrial Physics Department, Nnamdi Azikiwe University, Nigeria

*E-mail: jeruaye@gmail.com

Received 25 October 2018, accepted 6 December 2018

Europium-doped MgSe films were deposited via electric field-assisted spray pyrolysis. The dopant concentration of the bulk solution of europium trioxide was 5wt. %. However, for doping the films at different substrate temperatures, volume percentage (vol. %) was employed at each instance of variation. Variation of spray temperature was around 573K and 673K (± 0.3). Deposition occurred at optimized conditions. Spectra of absorption indicate poor absorption characteristics demonstrated by Europium-doped MgSe films in the ultra-violet region and very low absorption characteristics in the visible section. Absorption peaks were evident around 230nm, 240nm, 350nm and 365nm which confirmed defect states are inherent inside the crystal structure of the films. The films displayed high transparency and low reflection in the visible section at varying substrate temperatures. The high transparency revealed by the MgSe:Eu films in the visible section of the electromagnetic spectrum makes the material applicable as a coating layer in the manufacturing of transparent products. Band gap energies within the range of 2.49eV to 2.95eV corresponding to varying substrate temperatures (573K, 598K, 623K, 648K and 673K) and film thicknesses (2900nm, 2750nm, 2500nm, 2100nm and 200nm) were determined for the MgSe:Eu films. However, a clear observation shows that the band gaps of MgSe:Eu films are mainly dependent on thickness such that the obtained band gaps decreased with increasing thickness (band gap increases with thickness reduction). Structural analysis (XRD) studied at 10% and 40% Eu concentrations reveals a hexagonal (or wurzite) structure for the films with a distortion in crystallinity at higher dopant concentration (40 vol. %) and a resultant blue shift in the lattice constant from the bulk value. Multiple planes of reflection from XRD pattern of the deposited MgSe:Eu films indicate clearly that the films are polycrystalline. Surface morphology (SEM) confirms the highly strained nature and the presence of defect states within the crystal lattice of the Europium-doped MgSe films. Composition of MgSe:Eu films obtained by energy dispersive analysis x-ray (EDAX) confirms the growth of MgSe:Eu films.

KEYWORDS: Magnesium Selenide, Spray Pyrolysis, Europium, Temperature, Structural, Films, Band gap.

РІСТ МАГНІЄВО-СЕЛЕНІДНИХ ПЛІВОК ЛЕГОВАНИХ ЄВРОПІЄМ МЕТОДОМ СПРЕЙ-ПІРОЛІЗУ В ЕЛЕКТРИЧНОМУ ПОЛІ: ОПТИЧНИЙ І СТРУКТУРНИЙ АНАЛІЗ

D.M. Jeroh, A.J. Ekpunobi, D.N. Okoli

Physics/Industrial Physics Department, Nnamdi Azikiwe University, Nigeria

Плівки MgSe леговані європієм формувалися за допомогою піролізу в електричному полі. Об'ємна концентрація домішки у розчині триоксиду європію становила 5 wt. %. Проте при легуванні плівок при різних температурах субстрату, кожного разу використовувався об'ємний відсоток (vol. %). Варіація температури наплення становила близько 573 K і 673 K ($\pm 0,3$). Осадження відбувалося в оптимізованих умовах. Спектри абсорбції свідчать про слабкі поглинальні характеристики, продемонстровані плівками, що містять оксид MgSe, в ультрафіолетовій області та дуже низькі характеристики поглинання у видимому діапазоні. Піки поглинання спостерігались навколо 230 нм, 240 нм, 350 нм та 365 нм, що підтверджує наявність дефектів всередині кристалічної структури плівок. Плівки демонстрували високу прозорість і низьку здатність до відбиття у видимому діапазоні при різних температурах підкладки. Висока прозорість, виявлена плівками MgSe:Eu у видимому діапазоні електромагнітного спектра, робить матеріал придатним у якості шару покриття для виготовлення прозорих виробів. Для плівок MgSe:Eu була визначена ширини енергетичної зони в межах від 2,49 до 2,95 еВ, що відповідає різним температурам підкладки (573 K, 598 K, 623 K, 648 K і 673 K) та товщин плівок (2900, 2750, 2500, 2100, 200 нм). Проте, спостереження чітко показує, що ширини енергетичної зони зразків плівок MgSe:Eu в основному залежать від товщини, так що отримані ширини енергетичної смуги зменшуються з збільшенням товщини (ширина смуги зростає із зменшенням товщини). Структурний аналіз (XRD), проведений для концентрацій 10% та 40% Eu, показує гексагональну (або вурцітну) структуру для плівок із порушенням кристалічності при більш високій концентрації домішки (40 об.%) і як наслідок синій зсув константи решітки порівняно з об'ємним значенням. Кілька площин відбиття від шару XRD нанесених плівок MgSe:Eu чітко показують, що плівки є полікристалічними. Поверхнева морфологія (SEM) підтверджує високу напруженість та наявність дефектних станів у кристалічній решітці плівок MgSe, що містять сплави Європію. Структура плівок MgSe: Eu, отриманих за допомогою енергетичного дисперсійного аналізу рентгенівського випромінювання (EDAX), підтверджує ріст плівок MgSe: Eu.

КЛЮЧОВІ СЛОВА: селенід магнію, спрей-піроліз, європій, температура, структура, плівки, ширина смуги

For decades, semiconductors have proven absolutely effective and reliable when it comes to designing and fabricating several electronic devices. Amongst the studied semiconductors, II-VI semiconductors have been widely reported in searching for novel materials toward advancing the study of semiconductors for various applications. As such, focus has shifted to the inclusion of magnetic and rare-earth ions into pure semiconductors to explore their variable properties. The alkaline earth chalcogenides such as MgSe, CaSe, SrSe, etc., have attracted scientists perhaps due to their potential applications in various optoelectronic devices, especially luminescent ones [1]. Magnesium is located in group IIA and when combined with selenium, it can be classified as a II-VI semiconductor. Due to its

hygroscopic nature and unstable zinc-blende structure, a detailed investigation on the physical properties of MgSe is not clear till now and only few reports are existent in the literature [2].

Magnesium selenide (MgSe) films have previously been produced by spray pyrolysis [1-4], solution growth technique [5-7], molecular beam epitaxy [8-9], metal-organic chemical vapour deposition [10], metal-organic vapour-phase epitaxy [11]. In our current research, spray pyrolysis (SP) based on electrostatic field was used to deposit magnesium selenide with europium as dopant (MgSe:Eu) and a careful analysis of its optical and structural parameters are presented. SP was considered due to its advantages as reported by [12].

The major aim of this study is to introduce a pinch of europium (as a dopant) into MgSe and study its optical and structural characteristics for possible applications of the material. This became necessary as only few reports are available on the optical and structural parameters of MgSe films and also the inclusion of rare-earth ions (Europium) in magnesium selenide films has not been described in available literatures. This research aims to close the gap by investigating the optical and structural parameters of only Europium-doped magnesium selenide films and possibly suggest applications of the films based on their determined characteristics.

EXPERIMENTAL DETAILS

The spray content of MgSe:Eu films comprises 1.8ml of 0.2M of magnesium acetate, 6ml of 0.2M of selenium dioxide (SeO_2) and 0.2ml of europium trioxide; Eu_2O_3 (0.1M concentration). 10% Dopant concentration (Vol. %) was considered for temperature variation. The resulting mixture was whisked for 25minutes by a magnetic stirrer. Due to swift precipitation of the mixture, the spray content was stabilized with the addition of some proportions of hydrochloric acid (concentrated). This was done to reduce the reaction pace of the mixture. Once homogeneity of the mixture was attained, it was sprayed via a syringe pump by spray pyrolysis (electrostatic) on the hot glass substrates maintained at 573K, 598K, 623K, 648K and 673K respectively. Distance optimization between the nozzle and substrate was achieved at 4.7mm, solution flow-rate was maintained at 2400 $\mu\text{L/hr}$ while time of deposition was maintained at 10minutes. The voltage throughout the whole deposition process was constant (optimized) at about 5.5kV.

RESULTS/DISCUSSIONS

Optical parameters

The film thickness was obtained by surface profile analysis using a DekTak Veeco 150 Stylus Surface Profiler. The absorbance spectra for MgSe:Eu films obtained at varying deposition temperatures are displayed in Figure 1.

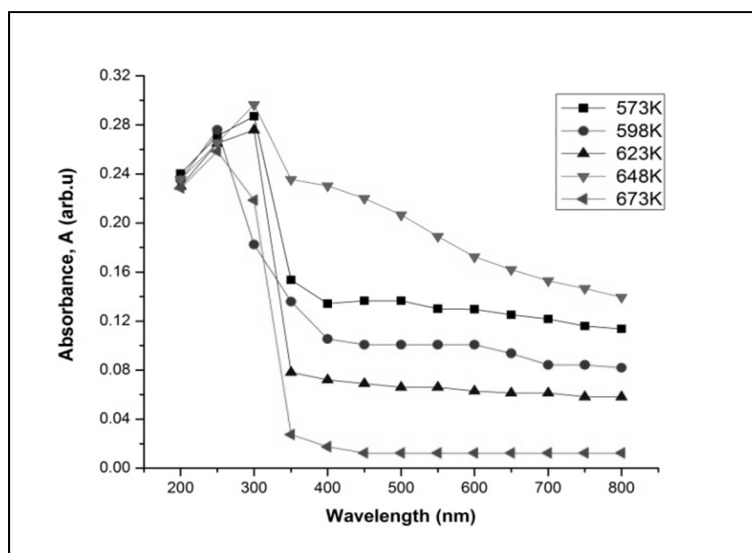


Fig. 1. Absorbance Spectra of MgSe:Eu Films at Varying Substrate Temperatures

Very poor absorption of light is obvious for the MgSe:Eu films at long wavelengths. Highest absorbance recorded is about 29.66% and was obtained at 648K in the ultra-violet region. Absorption peaks are evident around 230 nm, 240 nm, 350 nm and 365 nm. These observed peaks confirm defect states are inherent inside the crystal structure of the films. The low absorption of light revealed by the MgSe:Eu films suggests that more light will be transmitted by the material. An observation of Figure 1 indicates that the absorbance of the MgSe:Eu films decreases as temperature increases from 573K to 623K in the visible region. At 643K, there was a sudden increase in absorbance with further decrease of absorption as deposition temperature attains 673K. This behaviour could be as a result of defect states or strains present within the material which is responsible for the slight distortion of trend. Notwithstanding, it could be concluded that absorption decreases with increment in temperature in the visible zone. From the SEM results (Figures 6 a,b), cracks are observed on the surface of the films which is an indication that the films are highly strained

and the confirmation of defect states within the crystal lattice. Thus the SEM and optical results are well correlated. The transmittance curves of MgSe:Eu films are displayed in Figure 2 for varying temperatures.

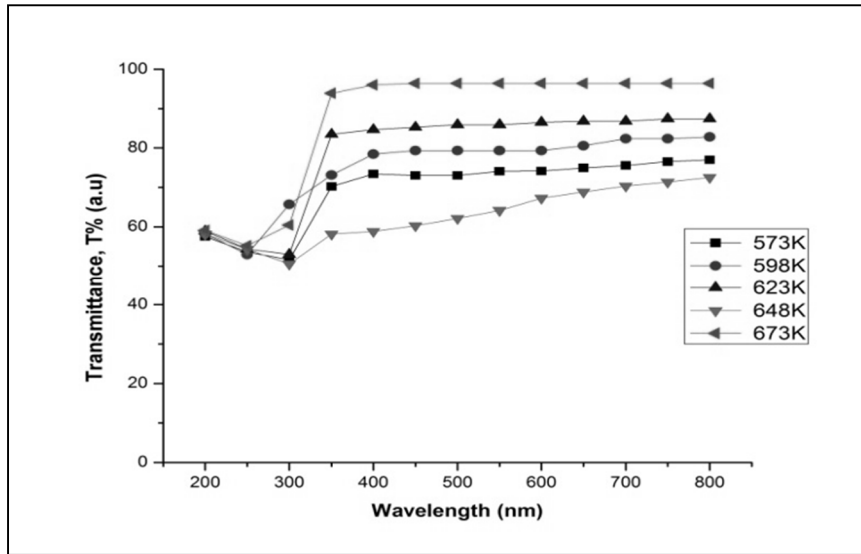


Fig. 2. Transmission Spectra for MgSe:Eu Films at Varying Substrate Temperatures

The transparency of the MgSe:Eu films improves with temperature from 573K up to 623K, slightly decreased at 648K and further increased at 673K. A careful inspection of all the films obtained at varying deposition conditions reveal high transparency around 73.42% and 96.47% in the visible region. The same reason adduced for the absorption results also applies to the transmittance results. This property of high transparency revealed by the MgSe:Eu films in the visible section of the electromagnetic spectrum makes the material applicable as a coating layer in the manufacture of transparent products.

The band gap (direct) energies of the MgSe:Eu films at varying deposition conditions were computed from the relation [13]:

$$(\alpha h\nu) = D (h\nu - E_g)^m \tag{1}$$

where D is a constant, m indicates the transition type. The value of m is assigned either 1/2 or 2 (for direct and indirect transitions respectively), E_g denotes energy of the band gap while $h\nu$ stands for energy of the photon.

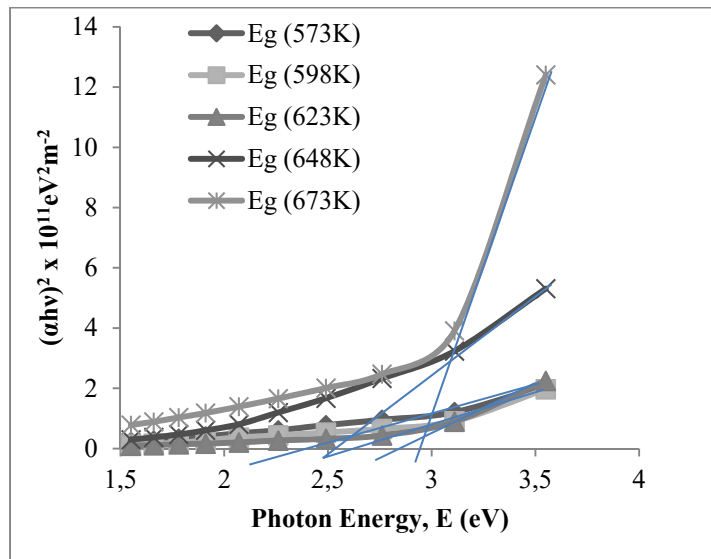


Fig. 3. Plot of $(\alpha h\nu)^2$ Versus Photon Energy for MgSe:Eu Films at Varying Substrate Temperatures.

The energy of band gaps of the films is within the range of 2.49eV to 2.95eV depending on the substrate temperature. The band gap energy is observed to increase slightly with temperature between 573K and 623K, reduces at 648 and further increased at 673K. However, a clear observation shows that the band gaps of MgSe:Eu films are mainly

dependent on thickness such that the obtained band gaps decreased with increasing thickness (band gap increases with thickness reduction).

Table 1a

Variation of Band Gap Energy with Substrate Temperature

Temperature (K)	Band Gap (eV)
573	2.65
598	2.75
623	2.85
648	2.49
673	2.95

Table 1b

Variation of Band Gap Energy with Thickness

Thickness (nm)	Band Gap (eV)
2900	2.49
2750	2.65
2500	2.75
2100	2.85
200	2.95

Table 1b reveals that a reduction in the thickness of the MgSe:Eu films caused a corresponding increment in band gap energy. Another notable observation is the fact that the MgSe:Eu film thickness was astronomically reduced at 673K. At the occurrence of this fact, the films were repeatedly deposited at this temperature a couple of times with variation of thickness still in the reported range. A very similar report has been given by [2], citing [14] wherein the various authors concluded that at higher temperatures there is a reduction in the transfer of precursor to the substrate. This, [2] and [14] attributed to gas convection emanating from the chamber, hence pushing away the droplets from the substrate surface leading to the development of crystallites within the vapour. Thickness of MgSe:Eu films were determined by profilometry using a DekTak Veeco 150 Profilometer.

STRUCTURAL CHARACTERIZATION OF MgSe:Eu FILMS X-RAY DIFFRACTION (XRD) ANALYSIS

The x-ray diffractogram of the Eu-doped MgSe films obtained at a deposition temperature of 623K, deposition time of 10 mins and 10% dopant concentration is displayed in Figure 4.

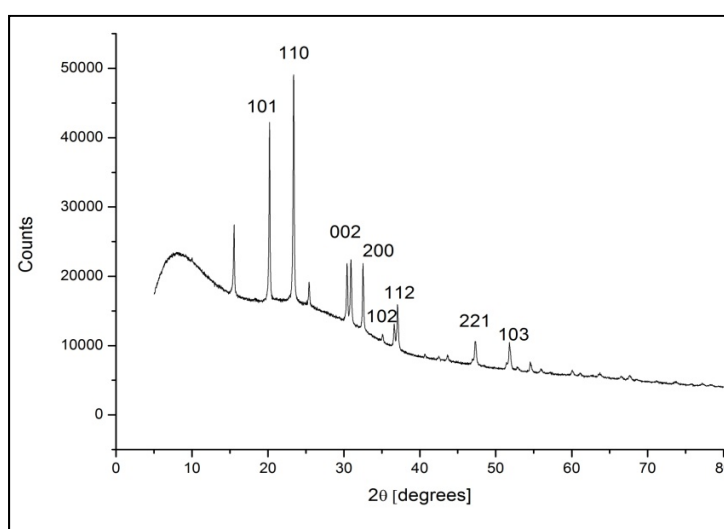


Fig. 4. XRD Diffractogram of MgSe:Eu Films at 623K and 10% Dopant Concentration.

Figure 4 reveals multiple planes of reflection from the XRD pattern of the deposited MgSe:Eu films. This indicates clearly that the films are polycrystalline. These diffraction patterns are indexed to the [101], [110], [002], [200], [102], [112], [221] and [103] planes having corresponding 2θ values: 20.37°, 23.53°, 30.67°, 32.68°, 36.77°,

37.21°, 47.43° and 51.97° respectively. The indexed planes clearly suggests a hexagonal structure for the MgSe:Eu films. The peak at 2θ equals 23.53° recorded the highest intensity indicating the preferred growth angle which has been indexed to the [110] plane. The lattice constant for the [110] plane was estimated to be about 5.3427Å which is lower than the reported standard value (5.462Å) published by NBS Monograph 25, section 5 (card no.: 53-61386) [15] for MgSe films.

In this research, optical studies reveal a blue-shift in band gap energy for the studied MgSe:Eu films while structural analysis shows the lattice constant (5.3427Å) is red-shifted from the bulk (5.462Å). It is to be emphasized that a reduction in the inter-atomic distance brings about a decrease in lattice constant. The implication of this is an increment in binding force between the valence electrons and parent atoms. Thus, as the valence electrons become more bound as a result of the decrease in inter-atomic spacing, more energy will be needed to free the valence electrons and move them into the conduction band to become free electrons. Thus a reduction of the lattice constant will result in an increase in the band gap energy. Thus, our structural and optical results are well correlated.

For an effective study of the structural details, parameters such as the grain size, inter-planar distance, strain, lattice constant, dislocation density and number of crystallites per unit area have been estimated and displayed in Table 2b.

The grain size, D, was estimated from the Debye-Scherrer expression [2, 16-17]:

$$D = \frac{0.94\lambda}{\beta \cos\theta} \quad (1)$$

where λ (1.540593Å) is the diffraction wavelength, β is the Full-Width at Half-Maximum (FWHM) while θ is the Bragg's diffraction angle.

The grain/crystallite sizes of the MgSe:Eu films at the different planes presented were estimated to be 41.19nm, 46.15nm, 47.79nm, 48.56nm, 52.97nm, 54.81nm, 61.76nm and 70.92nm respectively.

The inter-planar distance, d, was estimated from the expression [16]:

$$d = \frac{\lambda}{2\sin\theta} \quad (2)$$

The strain, ε, was estimated from the expression [18]:

$$\varepsilon = \frac{\beta \cos\theta}{4} \quad (3)$$

The dislocation density, δ, was estimated from the mathematical expression [19-20]:

$$\delta = \frac{1}{D^2} \quad (4)$$

where D is the grain size.

The lattice constant for the hexagonal phase of MgSe:Eu was estimated from the relation given by [21-22]:

$$\frac{1}{d^2} = \frac{4}{3a^2} (h^2 + hk + k^2) + \frac{l^2}{c^2} \quad (5)$$

where a; is lattice constant, d is the inter-planar spacing and hkl represents the miller indices.

The number of crystallites per unit area was calculated using the relation [23-24]:

$$N = \frac{t}{D^3} \quad (6)$$

where t, is the thickness of the MgSe:Eu film and D is the crystallite size corresponding to each plane.

Table 2a

Diffraction Angles and FWHM Values for MgSe:Eu Films Deposited at 623K.

2θ	θ	Cos θ	FWHM β°	FWHM (Radians)	βCosθ
20.37	10.19	0.9842	0.1600	0.002793	0.002042
23.53	11.77	0.9790	0.1600	0.002793	0.002734
30.67	15.34	0.9644	0.1800	0.003142	0.003030
32.68	16.34	0.9596	0.1400	0.002444	0.002345
36.77	18.39	0.9490	0.1800	0.003142	0.002982
37.21	18.61	0.9477	0.1600	0.002793	0.002647
47.43	23.72	0.9156	0.2200	0.003840	0.003516
51.97	25.99	0.8989	0.2000	0.003491	0.003138

Table 2b

Lattice Parameters for MgSe:Eu Films Deposited at 623K.

D (nm)	d (Å)	ϵ ($\times 10^{-4}$)	δ ($\times 10^{14}$ lines/m ²)	a (Å)	N ($\times 10^{15}$)	hkl
70.92	4.3562	5.1050	1.9882	6.1606	7.71	101
52.97	3.7779	6.8350	3.5640	5.3427	18.50	110
47.79	2.9127	7.5750	4.3785	5.8254	25.20	002
61.76	2.7380	5.8625	2.6217	5.4760	11.67	200
48.56	2.4423	7.4550	4.2408	5.4612	24.02	102
54.81	2.4144	6.6175	3.3287	5.9141	16.70	112
41.19	1.9153	8.7900	5.8941	5.7459	39.35	221
46.15	1.7581	7.8450	4.6952	5.5596	27.98	103

The diffractogram of Eu-doped MgSe films obtained at 623K, 10mins deposition time and 40% dopant concentration is displayed in Figure 5.

The reflections are indexed to [101], [110], [002] and [200] planes which clearly indicates a hexagonal structure for the film. The reflection angles corresponding to the indexed planes have 2 θ values at 20.26°, 23.43°, 30.46° and 32.57° respectively. The lattice constant of the preferred growth plane was estimated to be about 5.3652Å. The estimated lattice constant (5.3652Å) is close to the reported standard value (5.462Å) for MgSe films according to NBS, card no.: 53-61386 [15].

By comparison of Figures 4 and 5, it is observed that the number of prominent peaks decreased substantially when the dopant concentration was increased to 40%. This implies that the material losses its crystallinity at increased dopant concentration, thereby distorting the crystal structure of the material.

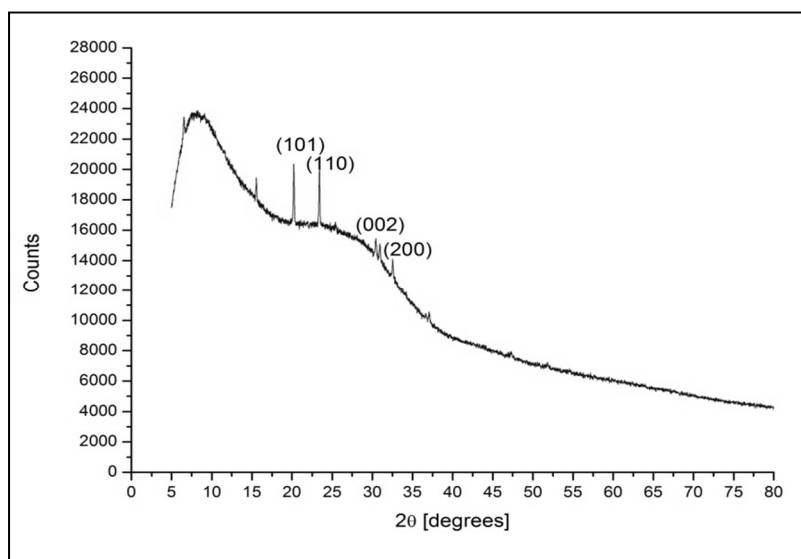


Fig. 5. XRD Diffractogram of MgSe:Eu Films at 623K and 40% Dopant Concentration.

Table 3a

Diffraction Angles and FWHM Values for MgSe:Eu Films Deposited at 623K, 40%.

2 θ	θ	Cos θ	FWHM β°	FWHM (Radians)	$\beta \text{Cos}\theta$
20.26	10.13	0.9844	0.1200	0.002094	0.002061
23.43	11.72	0.9792	0.1200	0.002094	0.002051
30.46	15.23	0.9649	0.1600	0.002793	0.002695
32.57	16.29	0.9599	0.1400	0.002444	0.002346

Table 3b

Lattice Parameters for MgSe:Eu Films Deposited at 623K, 40%.

D (nm)	d (Å)	ϵ ($\times 10^{-4}$)	δ ($\times 10^{14}$ lines/m ²)	a (Å)	N ($\times 10^{15}$)	hkl
70.26	4.3796	5.1525	2.0257	6.1937	8.650	101
70.61	3.7938	5.1275	2.0057	5.3652	8.522	110
53.73	2.9323	6.7375	3.4639	5.8646	19.341	002
61.73	2.7500	5.8650	2.6243	5.5000	12.754	200

SCANNING ELECTRON MICROSCOPY (SEM) STUDIES

The surface morphology of the MgSe:Eu films were studied at different conditions of growth and presented in Figures 6 (a-d).

From SEM images, cracks are evident all over the surface of the grown films (Figures 6(a-d) indicating that the films are highly strained). Such strains lead to defects within the crystal structure of the material. This is evident in the optical and XRD analysis.

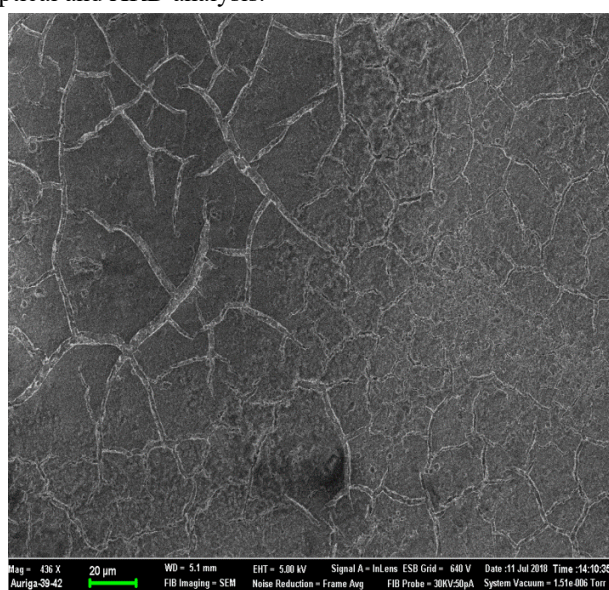


Fig. 6a. SEM Image of MgSe:Eu Films at 573K, 10mins and 10% Dopant Concentration.

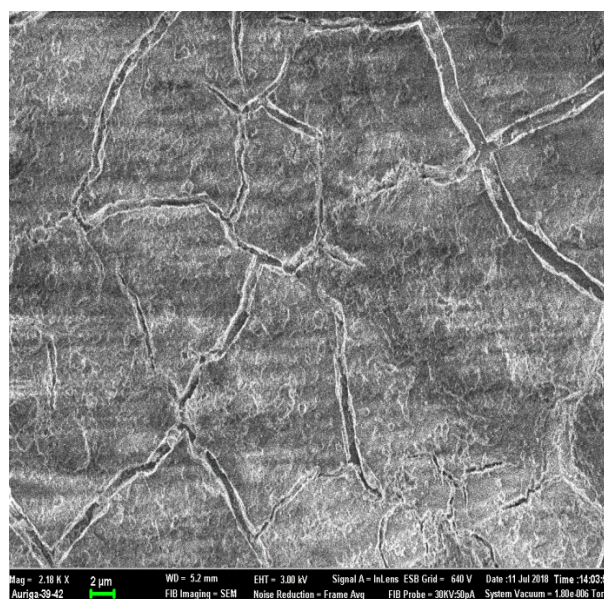


Fig. 6b. SEM Image of MgSe:Eu Films at 623K, 10mins and 40% Dopant Concentration.

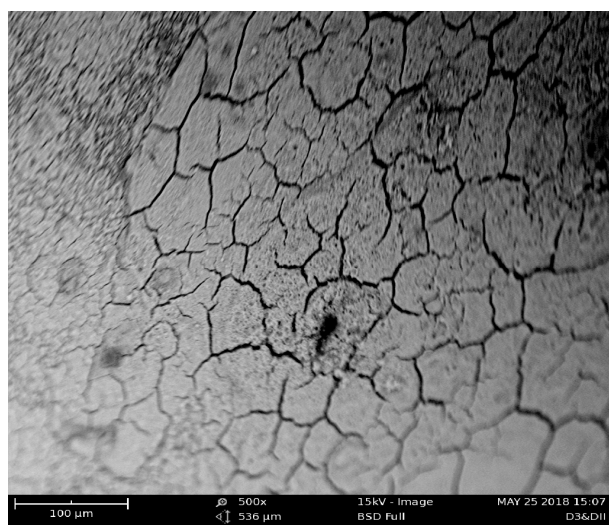


Fig. 6c. SEM Image of MgSe:Eu Film Obtained at 623K, 10mins, 10% Dopant Concentration at a Resolution of 500x.

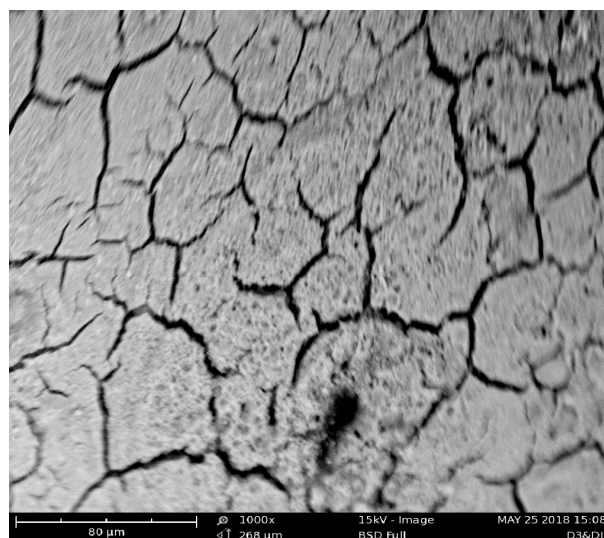


Fig. 6d. SEM Image of MgSe:Eu Film Obtained at 623K, 10mins, 10% Dopant Concentration at a Resolution of 1000x.

ELEMENTAL COMPOSITION

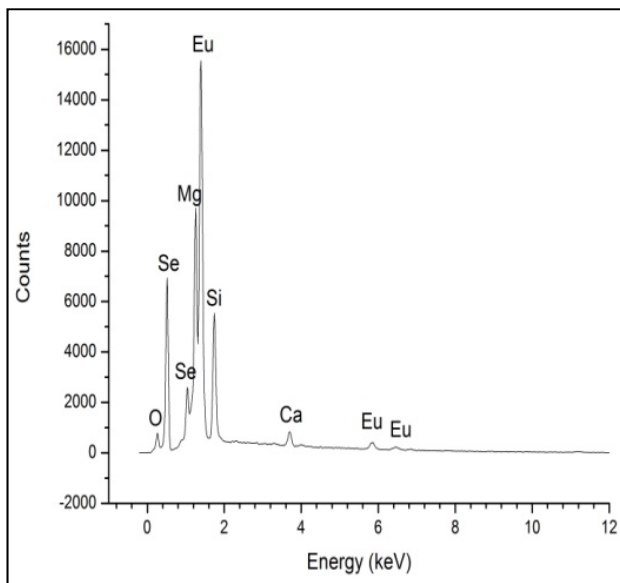


Fig. 7. EDX Spectrum of MgSe:Eu Films at 10% Eu Concentration and Growth Temperature of 573K.

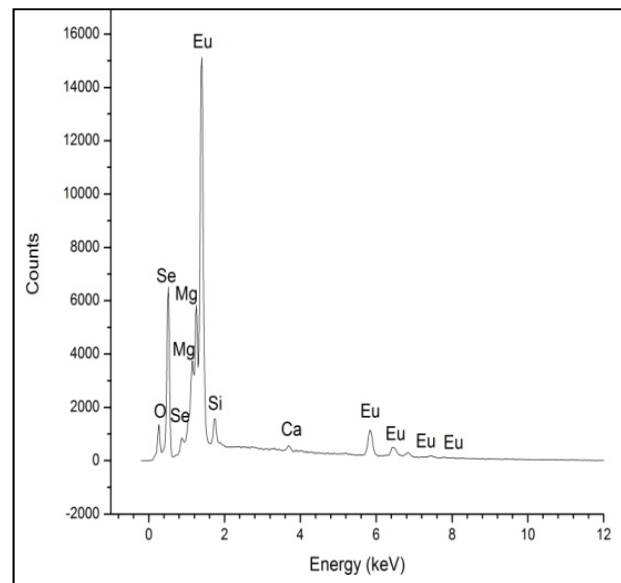


Fig. 8. EDX Spectrum of MgSe:Eu Films at 40% Eu Concentration and Growth Temperature of 623K.

To confirm the growth of MgSe:Eu films, energy dispersive analysis x-ray (EDX) spectroscopy was employed to ascertain the composition of the films. Figures 7 and 8 show the EDX spectrum of the MgSe:Eu films obtained at 10% and 40% Eu concentrations at growth temperatures of 573K and 623K. The presence of Mg, Se and Eu is obvious from the EDX spectrum confirming the formation of MgSe:Eu films. The presence of silicon (Si) and calcium (Ca) may have come from the glass substrate while the peak corresponding to oxygen (O) may be due to atmospheric exposure.

CONCLUSION

Thin films of MgSe:Eu with varying thicknesses obtained at varying substrate temperatures and dopant concentrations were obtained via electrostatic spray pyrolysis. The obtained band gap energies were discovered to be dependent on the film thickness. Strong blue-shift in band gap energy was observed for the MgSe:Eu films. Optical studies reveal the films will prove useful in creating optoelectronic devices and will also be valuable for coating materials that need to remain transparent. The XRD analysis conducted indicates hexagonal structure for the MgSe:Eu films while SEM analysis indicates the MgSe:Eu films are highly strained.

ACKNOWLEDGEMENT

The authors wish to appreciate the management and technicians at NAMIROCH laboratory, Abuja for assisting in conducting our research.

ORCID IDs

D.M. Jeroh  <https://orcid.org/0000-0002-1622-0337>

A.J. Ekpunobi  <https://orcid.org/0000-0002-5111-7298>

D.N. Okoli  <https://orcid.org/0000-0002-4196-8902>

REFERENCES

- [1]. Y.S. Sakhare, N.R. Thakare and A.U. Ubale, St. Petersburg Polytech. Uni. J. Phys. Math. **2**, 7-26 (2016).
- [2]. S.J. Gnanamuthu, S.J. Jeyakumar, A.R. Balu, K. Usharani and V.S. Nagarethinam, Int. J. Thin Fil. Sci. Tech. **2**, 121-123 (2015).
- [3]. Y.S. Sakhare, N.R. Thakare and A.U. Ubale, Arch. Phys. Res. **6**, 12-20 (2015).
- [4]. A.U. Ubale, Y.S. Sakhare, Vacuum. **99**, 124 (2014).
- [5]. A.U. Ubale, Y.S. Sakhare, Mater. Sci. Semicond. Process. **16**, 1769 (2013).
- [6]. A.U. Ubale, Y.S. Sakhare, S.G. Ibrahim and M.R. Belkhedkar, Solid State Sci. **23**, 96-108 (2013).
- [7]. A.U. Ubale, Y.S. Sakhare, Ind. J. Phys. **87**, 1183-1188 (2013).
- [8]. H.M. Wang, J.H. Chang, T. Hanada, K. Arai and T. Yao, J. Cryst. Growth. **208**, 253-258 (2000).
- [9]. P.X. Feng, J.D. Riley, R.C.G. Leckey and L. Ley, J. Phys.: Appl. Phys. D. **34**, 1293-1300 (2001).
- [10]. F. Jiang, Q. Liao, G. Fan, C. Xiong, X. Peng, C. Pan and N. Liu, J. Cryst. Growth. **183**, 289-293 (1998).
- [11]. P. Prete, N. Lovergine, L. Tapfer, C.Z. Fregonara and A.M. Mancini, J. Cryst. Growth. **214-215**, 119-124 (2000).
- [12]. M.D. Jeroh, A.J. Ekpunobi, D.N. Okoli, J. Nano- Electron. Phys. **10**, 03006-1 (2018).
- [13]. D.H. Hwang, J.H. Ahn, K.N. Hui, K.S. Hui and Y.G. Son, Nanoscale Res. Letts. **7**, 26 (2012).
- [14]. M Suganya, A.R. Balu and K. Usharani, Mater Sci Poland. **3**, 448-456 (2014).

- [15]. *Standard X-ray Diffraction Powder Patterns. National Bureau of Standards Monograph, 25 - Section 5*, (US Department of Commerce, Washington, 1967).
- [16]. N.J.S. Kissinger, M. Jayachandran, K. Perumal and C.S. Raja, *Bull. Mater. Sci.* **3**, 547-551 (2007).
- [17]. R.S. Meshram, R.M. Thombre, *Int. J. Adv. Sci. Eng. Technol.* **1**, 161-170 (2015).
- [18]. S. Muthumari, G. Devi, P. Revathi and R. Vijayalakshmi, *J. Appl. Sci.* **12**, 1722-1725 (2012). doi: 10.3923/jas.2012.1722.1725
- [19]. J. Pla, M. Tamasi, R. Rizzolt, M. Losurdo, E. Centurioni, C. Summonte and F. Rubinelli, *Thin Solid Films.* **425**, 185-192 (2003).
- [20]. Y.Z. Dawood, M.H. Hassoni and M.S. Mohamad, *Int. J. Pure. Appl. Phys.* **2**, 1-7 (2014).
- [21]. N.J.S. Kissinger, J. Suthagar, B.S. Kumar, T. Balasubramaniram and K. Perumal, *Acta. Phys. Pol. A.* **118**, 623-628 (2010).
- [22]. V.D. Mote, J.S. Dargad and B.N. Dole, *Nanosci. Nanoeng.* **1**, 116-122 (2013). doi: 10.13189/nn.2013.010204
- [23]. Z.R. Khan, M. Zulfequar and M.S. Khan, *Mater. Sci. Eng. B.* **174**, P.145-149 (2010).
- [24]. S.A. Aly, A.A. Akl and H. Howari, *Acta. Phys. Pol. A.* **128**, 414-418 (2015). doi: 10.12693/APhysPolA.128.414